Supporting Information:

Multiple-design and synergism toward superhigh capacitive energy storage $(Bi_{0.5}K_{0.5})TiO_3$-based lead-free superparaelectrics

Xinyao Li, [a #] *Jiachen Xi,* [a #] *Chongyang Li,* [a] *Wangfeng Bai,* [a*] *Shiting Wu,* [a] *Peng Zheng,* [c] *Peng Li,* [b] *Jiwei Zhai* [d*]

[#] These authors contributed equally: *Xinyao Li* and *Jiachen Xi*

[a] College of Materials and Environmental Engineering, Hangzhou Dianzi University, Hangzhou, 310018, China. E-mail: bwfcxj@126.com (Wangfeng Bai)

[b] School of Materials Science and Engineering, Liaocheng University, Liaocheng, 252059, China

[c] College of Electronics and Information, Hangzhou Dianzi University, Hangzhou, 310018, China.

[d] Functional Materials Research Laboratory, School of Materials Science & Engineering, Tongji University, No. 4800 Caoan Highway, Shanghai, 201804, China. E-mail: apzhai@tongji.edu.cn (Jiwei Zhai)

Experimental section

Sample preparation:

(1-x)($K_{0.5}Bi_{0.5}$)TiO_3-x$CaTiO_3$ (denoted as BKT-xCT, x=0, 0.1, 0.3, 0.5) were synthesized via a conventional solid-state method. High-purity Bi_2O_3, K_2CO_3, TiO_2, $CaCO_3$ (≥ 99%) powders were used as raw powders. The stoichiometrically weighed powders were mixed by ball milling in ethanol for 24 h and then dried at 110 °C for 6h. The obtained BKT and CT powders were calcined at 900 °C for 6 h and 1000°C for 3h in an air atmosphere, respectively. The resulting calcined powders were weighed based on the compositions and then milled again. The dried powders with 8 wt% PVA were pressed into pellets with a diameter of 10 mm. Finally, the ceramic samples were obtained via sintering pellets at 1050-1150 °C for 4h in air. To conduct energy storage measurements, the sample thickness was thinned and polished to ~ 50-70 μm and then gold electrodes with an area of ~ 0.00785 cm^2 (~ 1 mm in diameter) were fabricated by ion sputtering.

Electrical properties:

The dielectric response and impedance spectroscopy of the ceramics with sliver electrodes on polished surfaces were examined by a high-precision LCR meter (HP 4990 A; Agilent, Palo Alto, CA). The temperature/frequency/cycles-dependent *P-E* loops and FORC curves were measured by a ferroelectric analyzer (RT1-Premier II, Radiant Technologies InC, USA) to evaluate the energy storage capacity. The charging-discharging performance was evaluated by a commercial charge-discharge platform (CFD-003, Gogo Instruments Technology, China). To obtain the Vickers hardness, the ceramic was polished to a thickness of ~ 0.1 cm and then conducted under a load of 4.9033 N for 15 s using a Vickers diamond indenter (FALCON 507, INNO-VATEST, the Netherlands). The absorption spectrum was determined using a UV-vis spectrophotometer (TU-1901, Puxi Instruments Technology, China) with an integrating sphere to achieve the band gap.

Structural characterization:

The phase structures and local structural information of samples were examined by X-ray diffraction (XRD) using a diffractometer with Cu Kα radiation (MiniFlex600, Rigaku, Japan) and Raman spectra using a Raman scattering spectrometer (Horiba/Jobin Yvon, Villeneuve d'Ascq, France). The morphology and elements distribution of the ceramics were recorded by Filed-emission scanning electron microscope (FE-SEM, S-4200, Hitachi, Tokyo, Japan), and the grain size of the ceramics was evaluated by a combination of Nano Measurer. The surface morphology, amplitude, and phase signals of well-polished ceramics were characterized by PFM using atomic force microscopy with an ac voltage amplitude of 2.5 V and frequency of 380 kHz (MFP-3D, Asylum Research, USA). The domain morphology was determined by field-emission transmission electron microscope (TEM, FEI Talos F200X, USA) operated at 200 kV. The TEM sample was prepared by a typical process combining mechanical thinning, polishing, and finally ion milling system (Gatan 695, USA).

The FORC distribution：

In this work, E_{max} is set to be 80 kV/cm, $\Delta\alpha = \Delta\beta = \Delta E = 3.2$ kV/cm. An approximate method to calculate $p(\alpha,\beta)$ is

$$p(\alpha,\beta) = \frac{1}{2}\frac{\partial P^2(\alpha,\beta)}{\partial\alpha\partial\beta} \#(1)$$

where $p(\alpha,\beta)$ is the polarization of the FORC loop, α is the reversal electric field, and β is the real electric field [1-4].

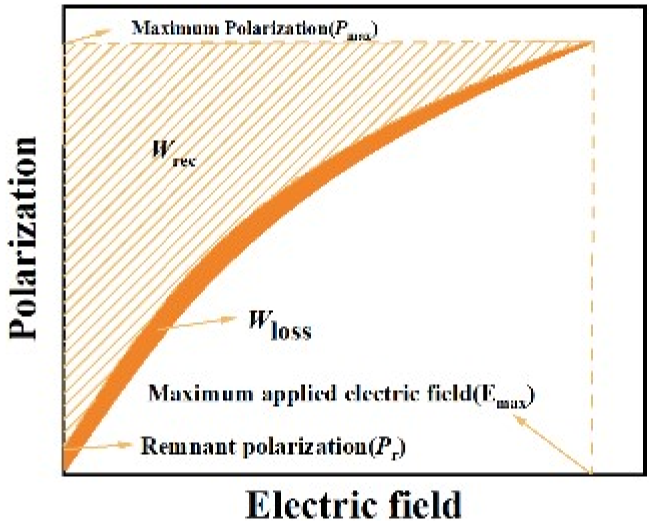

Figure S1. Sketch map of *P*-*E* hysteresis loop for the calculation of energy-storage parameters.

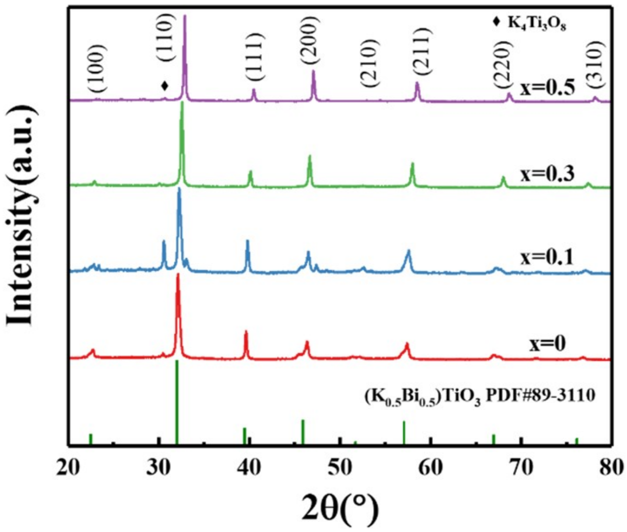

Figure S2. XRD patterns of the BKT-xCT ceramics.

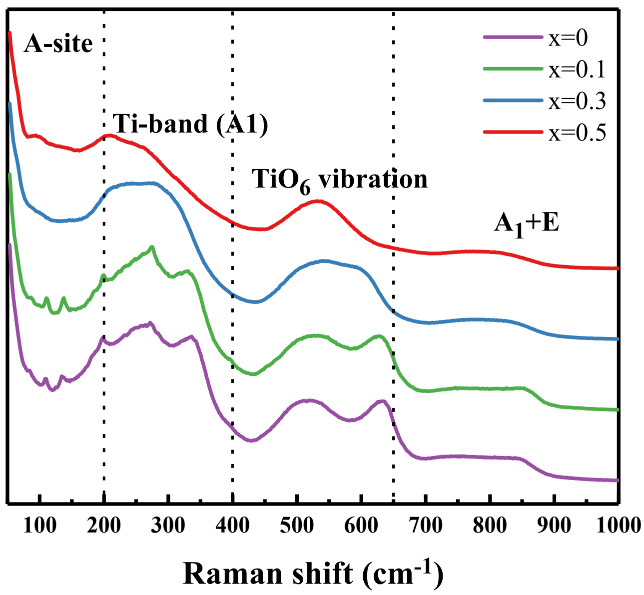

Figure S3. Raman spectra of the BKT-xCT ceramics.

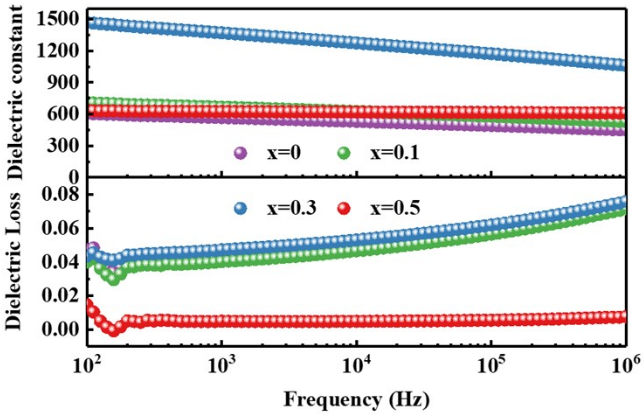

Figure S4. Room-temperature dielectric response as a function of frequency for the BKT-xCT ceramics.

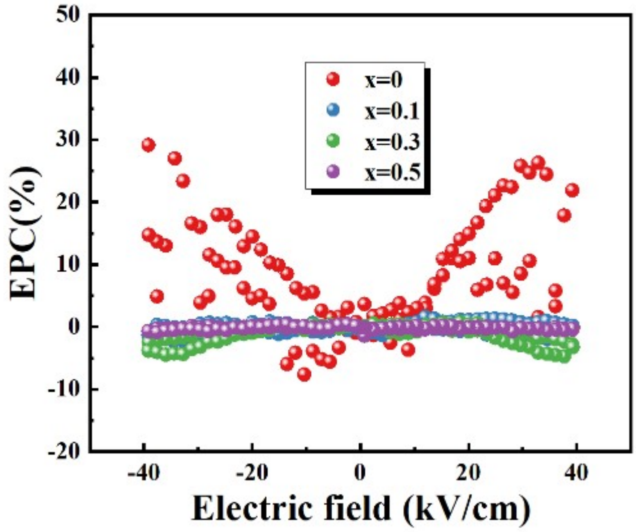

Figure S5. The change of dielectric constant for the BKT-xCT ceramics.

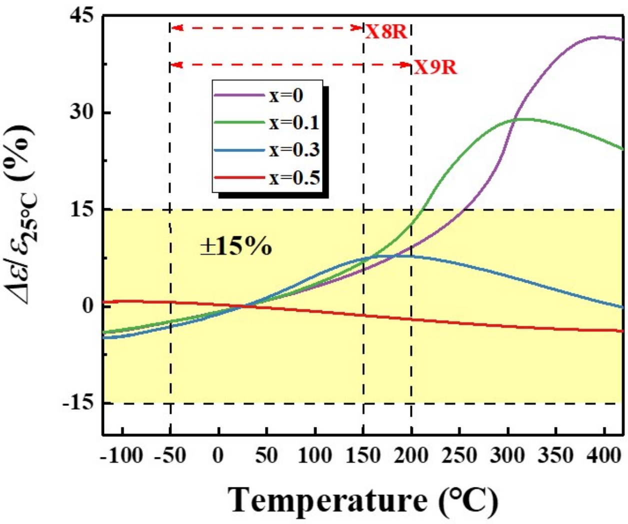

Figure S6. The normalized dielectric constant in a wide temperature range for the BKT-xCT ceramics.

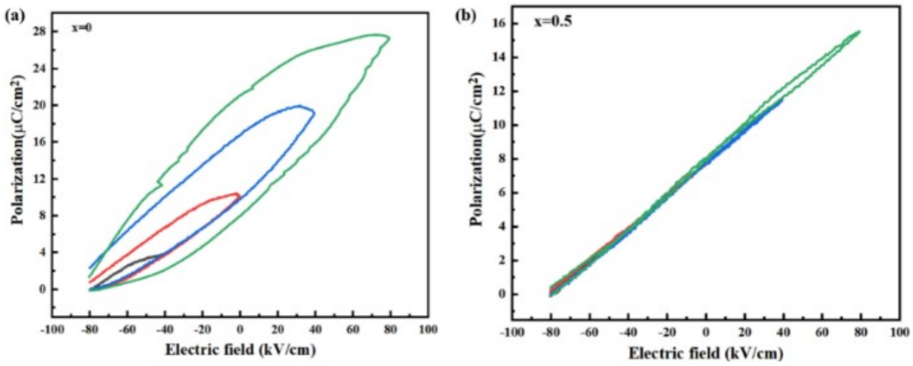

Figure S7. FORC curves for (a) BKT and (b) BKT-0.5CT ceramic.

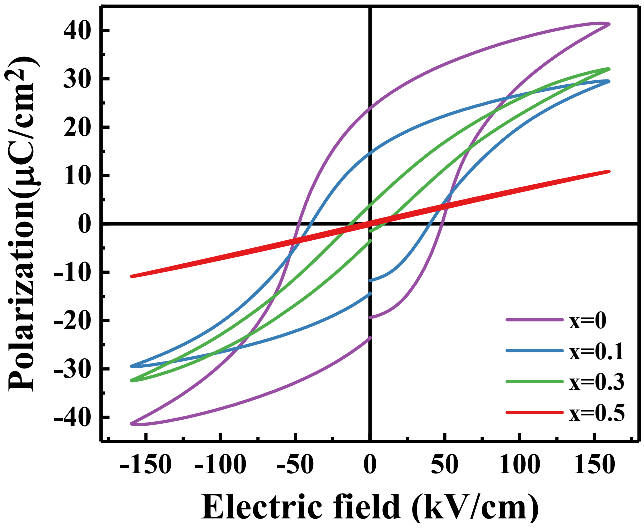

Figure S8. Bipolar *P-E* loops measured at room temperature and 160 kV/cm for BKT-xCT ceramics.

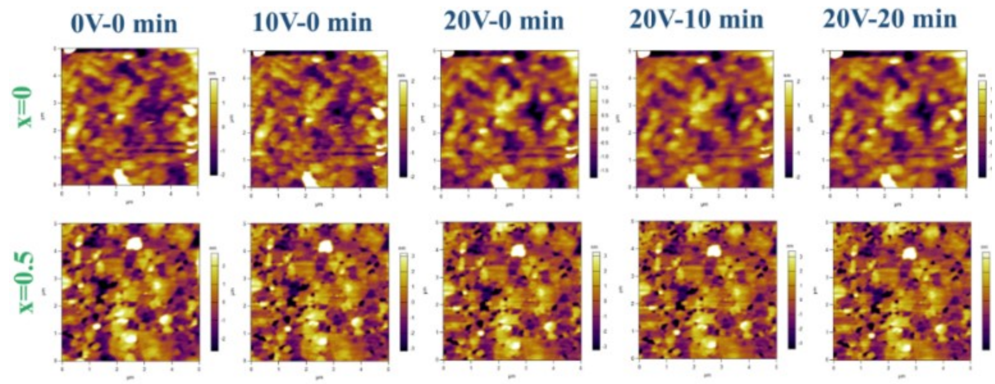

Figure S9. Out-of-plane PFM morphology under different voltage and relaxation durations for x = 0 and x = 0.5 ceramic.

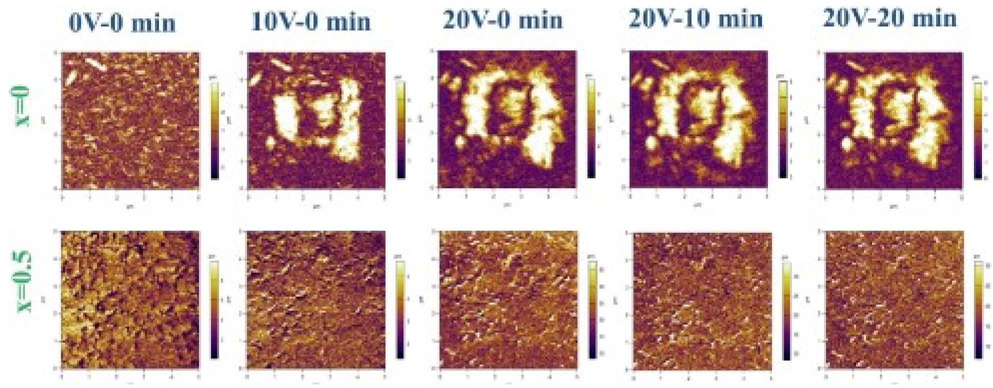

Figure S10. Out-of-plane PFM amplitude under different voltage and relaxation durations for x = 0 and x = 0.5 ceramic.

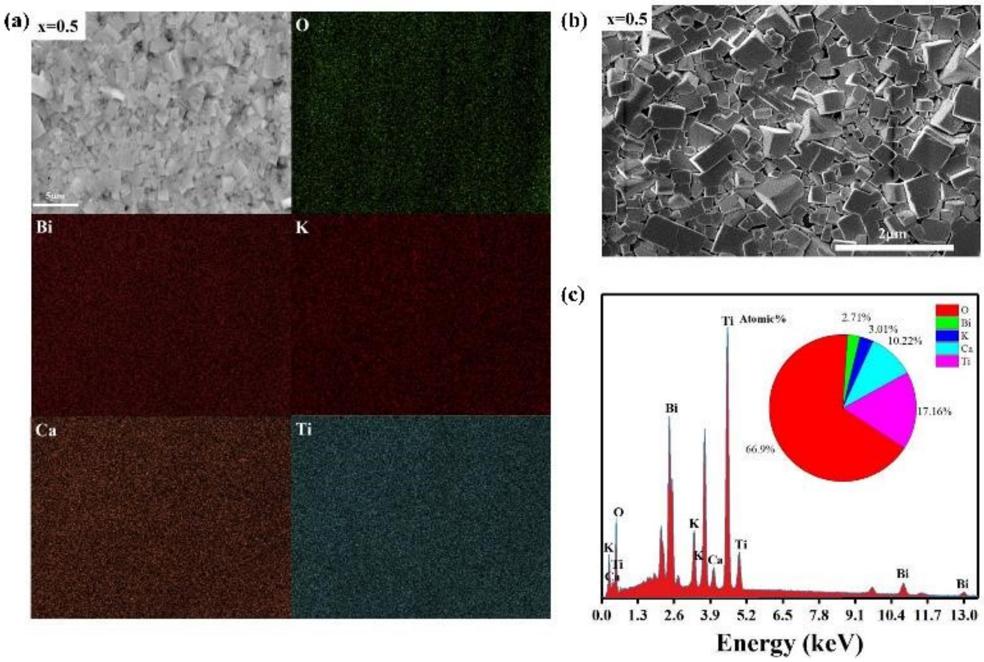

Figure S11. (a) Elements mapping, (b) surface SEM image, and (c) energy spectrum and atomic proportion of all elements for x=0.5 ceramic.

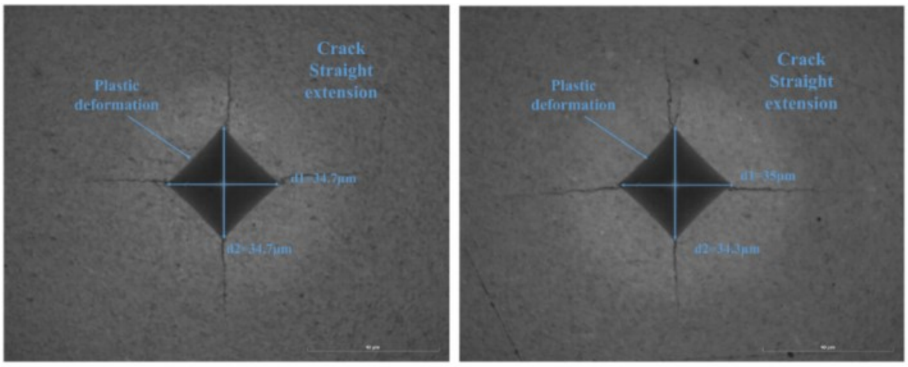

Figure S12. Surface patterns generated by Vickers diamond indenter for BKT-0.5CT ceramic.

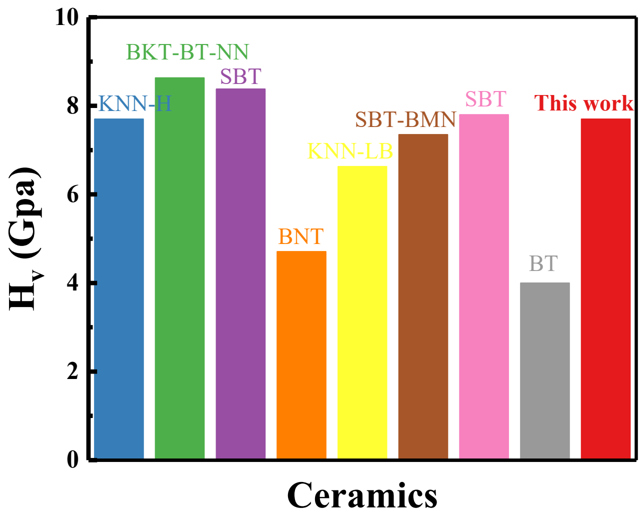

Figure S13. A comparison of H_v between BKT-0.5CT ceramic and some classic perovskite systems.

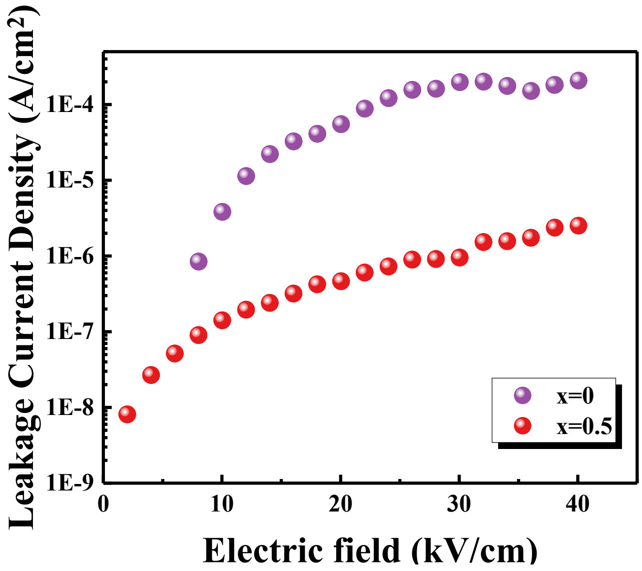

Figure S14. Leakage current density measured at 40 kV/cm for BKT and BKT-0.5CT ceramic.

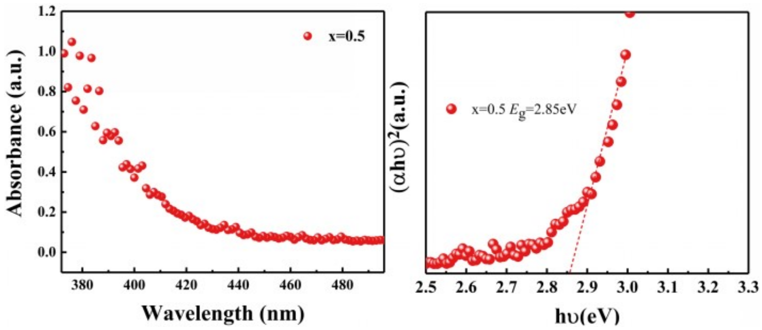

Figure S15. UV-vis absorbance spectra and $(\alpha h\nu)^2$ vs *hv* plot for BKT-0.5CT ceramic.

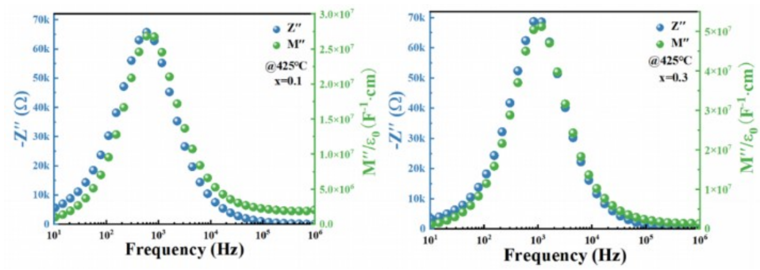

Figure S16. M″ spectroscopic plots at 425°C for x=0.1 and x=0.3 ceramic.

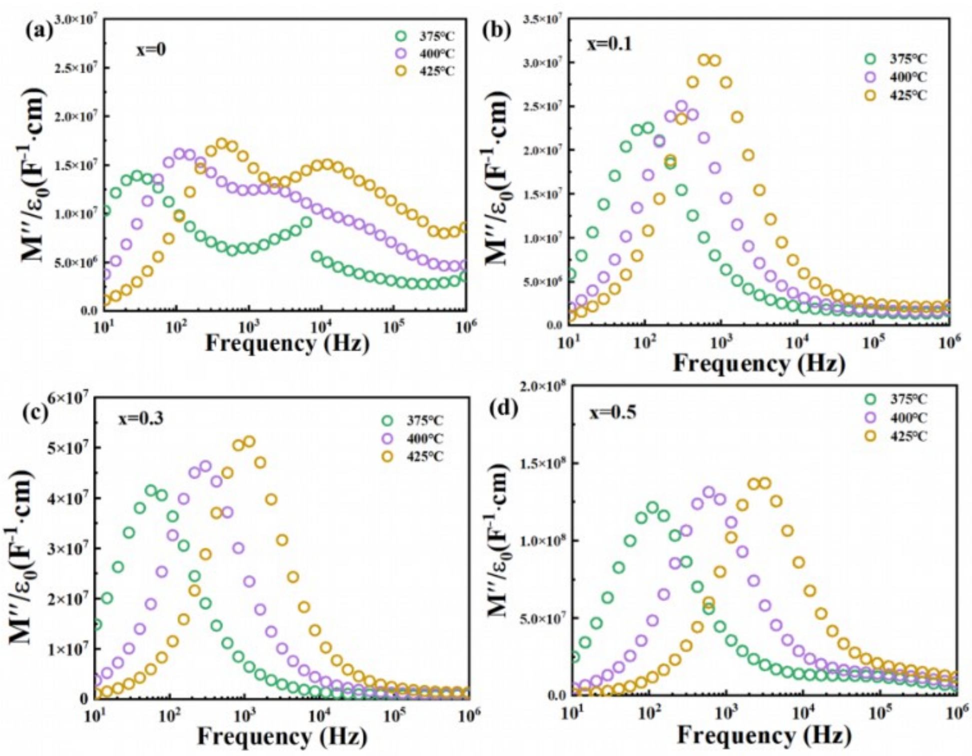

Figure S17. M″ spectroscopic plots at different temperature for BKT-xCT ceramics.

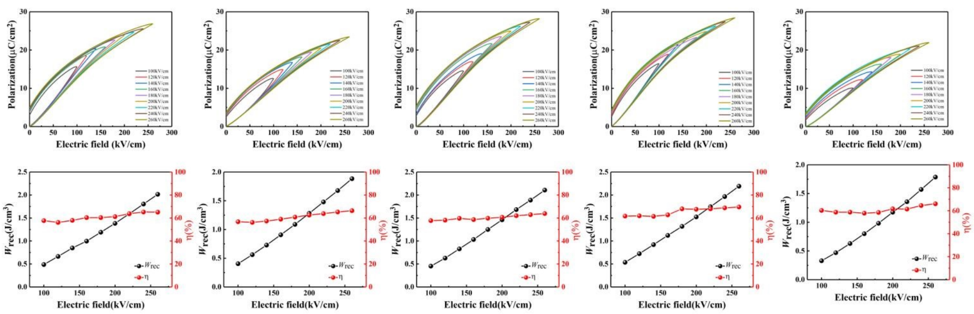

Figure S18. Five unipolar field-dependent *P-E* loops of pure BKT ceramic.

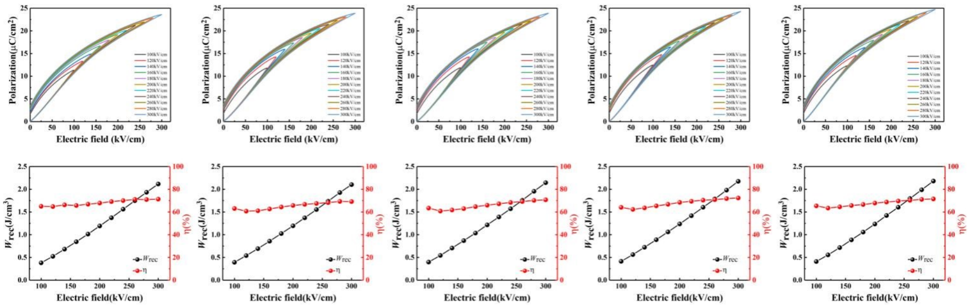

Figure S19. Five unipolar field-dependent *P-E* loops of BKT-0.1CT ceramic.

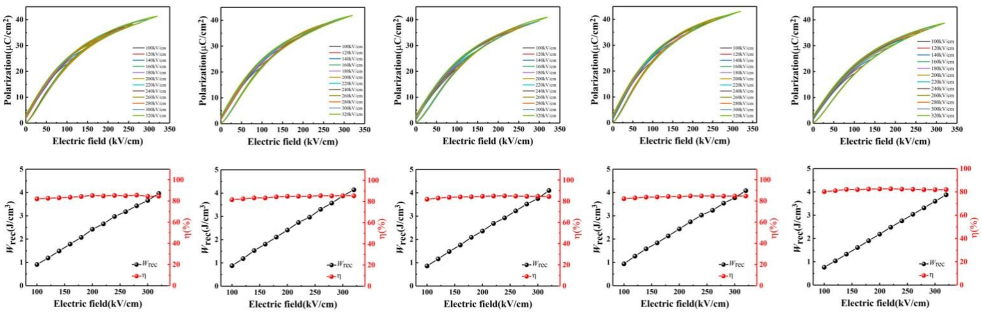

Figure S20. Five unipolar field-dependent *P-E* loops of BKT-0.3CT ceramic.

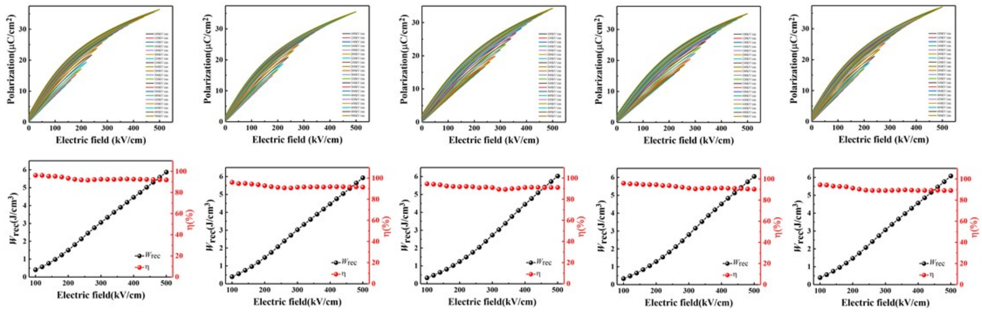

Figure S21. Five unipolar field-dependent *P-E* loops of BKT-0.5CT ceramic.

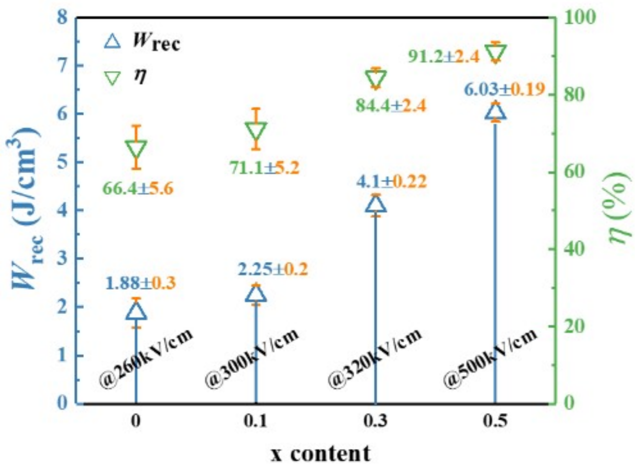

Figure S22. The change of W_{rec} and η near respective E_{b} for BKT-xCT ceramics.

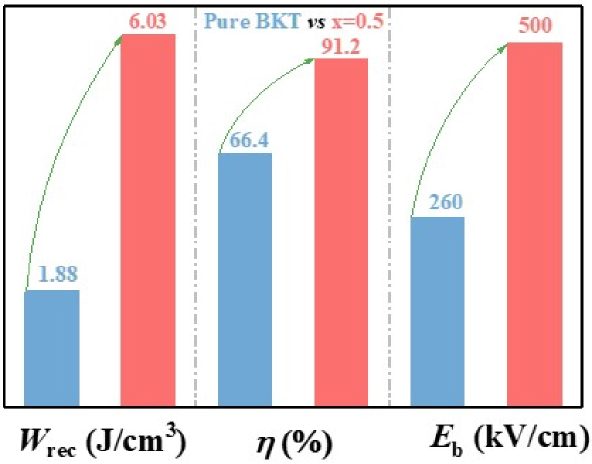

Figure S23. Comparison of energy storage performance in terms of W_{rec}, η, and E_b for pure BKT and BKT-0.5CT ceramic.

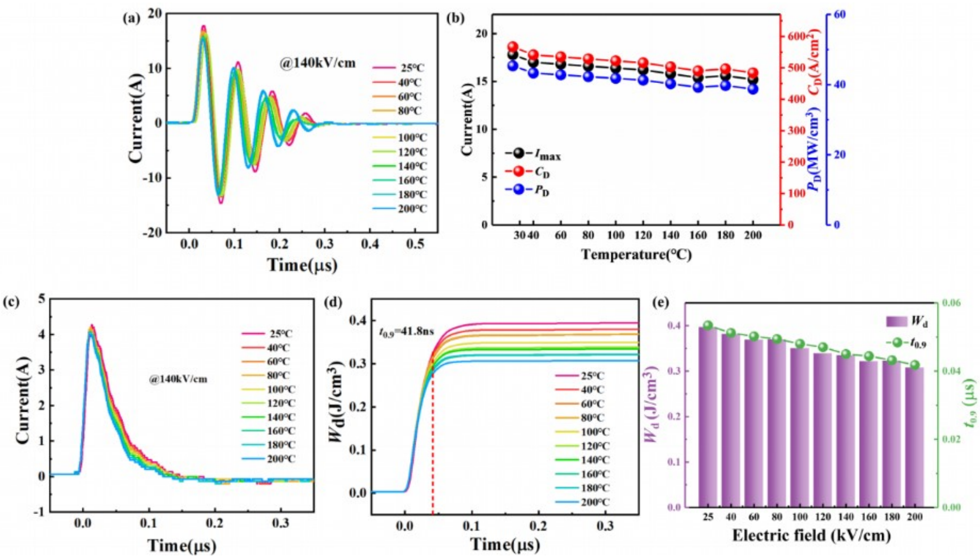

Figure S24. Temperature-dependent (a) underdamped discharge curves, (b) the change of I_{max}, C_D, and P_D, (c) overdamped discharge curves, (d) W_d-t curves, and (e) the variation of W_d and $t_{0.9}$ for BKT-0.5CT ceramic.

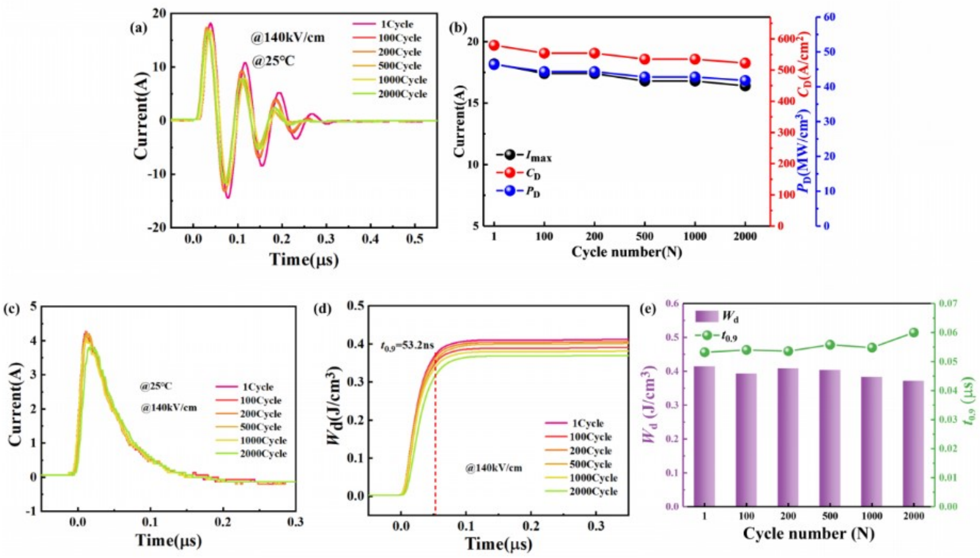

Figure S25. Cycles-dependent (a) underdamped discharge curves, (b) the change of I_{max}, C_D, and P_D, (c) overdamped discharge curves, (d) W_d-t curves, and (e) the variation of W_d and $t_{0.9}$ for BKT-0.5CT ceramic.

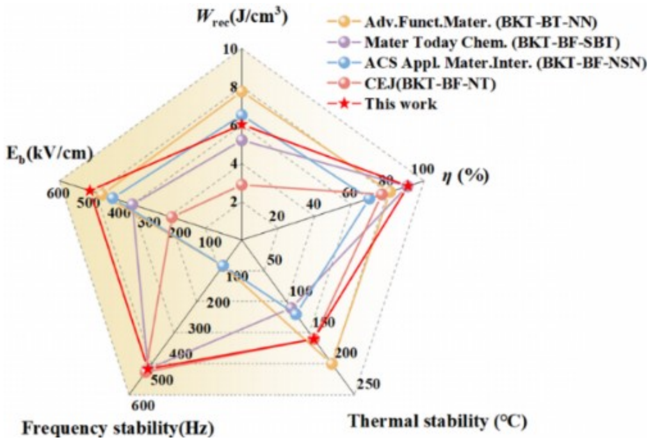

Figure S26. Comprehensive performance comparison of BKT-0.5CT and representative BKT-based energy storage ceramics in terms of W_{rec}, η, E_b, thermal stability, and frequency endurance.

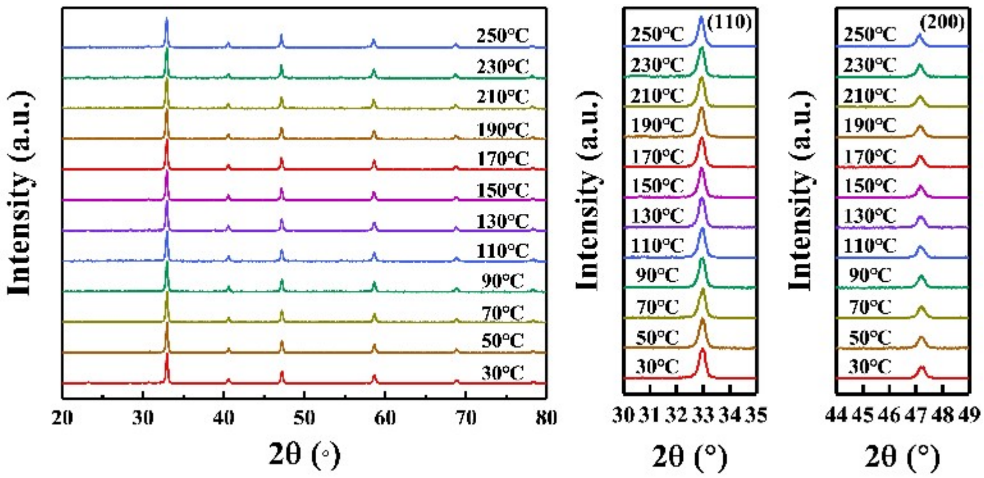

Figure S27. Temperature-dependent XRD patterns for BKT-0.5CT ceramic.

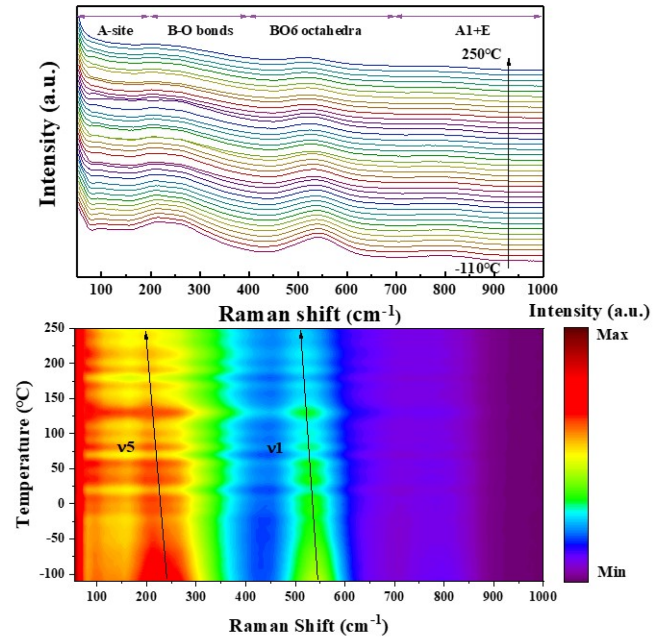

Figure S28. Raman spectra of the BKT-0.5CT ceramic measured from -110 ℃ to 250 ℃.

Table S1. A summarization of BKT-0.5CT ceramic and recently reported BKT-based energy storage ceramics in terms of E_b, W_{rec} and η.

Compositions	**E_b (kV/cm)**	**W_{rec} (J/cm^3)**	**η (%)**	**Ref.**
BKT-MLT	180	2.08	68	[5]
BKT-BMN	230	3.14	83.7	[6]
BKT-ST	190	2.31	77.7	[7]
BKT-BF-NT	150	2.88	76.9	[8]
BKT-ST-BZT	260	3.07	88	[9]
BKT-BT-NN	460	7.57	81.4	[10]
BKT-BF-SBT	360	5.21	90.87	[11]
BKT-BF-SMN	410	6.1	72	[12]
BKT-BF-NSN	425	6.52	70	[13]
KNBNTF	425	7.03	86	[14]
BKT-CT	**500**	**6.03**	**91.2**	**This work**

Table S2. Summarization of W_{rec}, E_b and η with various admirable lead-free energy storage ceramics with η of ≥ 90%.

Compositions	E_b (kV/cm)	W_{rec} (J/cm^3)	η (%)	Ref.
BNT-BAT-CT	440	5.81	97.8	15
BNT-SNA	520	6.64	96.5	16
KNN-BZT	600	6.7	92	17
BF-BT-BLH	520	6	90	18
BF-BT-BSZ	185	3.06	92	19
BF-BT-NN	360	8.12	90	20
BNT-SBT-KNN	290	3.72	90.7	21
BT-BMT	350	4.49	93	22
BNT-BZN	240	3.22	91.2	23
BNT-ST	535	5.63	94	24
BNT-SLT	338	4.14	92.2	25
NN-SBT	288	4.5	90.3	26
NN-BMT	800	8	90.4	27
CSTZ	440	3.37	96	28
CST-Mg	460	2.88	90	29
BKT-BF-CT	420	6.34	93.32	30
BKT-BF-SBT	360	5.21	90.87	11
BT-BZZ	250	2.47	94.4	31
BT-SBT-BMZ	370	4.03	96.2	32
BT-BLZ	285	3	93.8	33
BT-BMN	520	4.55	91	34
BF-SBT-SLT	260	2.55	92	35
CST-SiO	360	2	96	36
CT-BNT-BAT	700	6.39	94.4	37

CT-Sm	547	2	93.7	[38]
BT-BMS	240	2.25	94	[39]
SBT	290	2.1	97.6	[40]
SBT-BMH	360	3.1	93	[41]
SBT-BNN	340	3.71	97	[42]
BNT-SST	422	5.02	90	[43]
BNT-BZN	180	2.86	90	[23]
BNT-SBT-BMN	470	7.5	92	[44]
BT-BMZ	230	1.61	94.3	[45]
BT-BNT-SSN	206	2.02	90.18	[46]
BT-KNT	300	2.03	94.5	[47]
SBT-BZN	225	1.62	99.8	[48]
BKT-CT	**500**	**6.03**	**91.2**	**This work**

Table S3. Comparison of temperature stability between BKT-0.5CT and other representative lead-free energy storage ceramics.

Compositions	E (kV/cm)	W_{rec} (J/cm^3)	η (%)	T (°C)	Ref
BKT-BT-NN	300	4.31	86	200	[10]
ANT	400	4.3	91	150	[49]
BNT-BT-CLT	280	3.49	92.5	150	[50]
SBT-BMZ	200	1.6	92	150	[51]
BBT12	300	3.28	85.57	120	[52]
KNN-H	400	3.38	85.8	140	[53]
BNT-SST	250	2.5	84	180	[43]
BNT-ST	300	3	92	130	[24]
KNN-BNZ	350	2	89	160	[54]
BT-BMZ	300	2.85	87	150	[55]
ALN	320	2.5	90	120	[56]
BF-BT-SBT	250	3.2	75	120	[57]
KNN-BZNT	400	3.1	80	180	[58]
BF-ST	350	3.8	91	120	[59]
BKT-CT	**350**	**3.45**	**90.68**	**160**	**This work**

Table S4. Comparison of frequency endurance between BKT-0.5CT and other representative lead-free energy storage ceramics.

Compositions	***E* (kV/cm)**	**W_{rec} (J/cm^3)**	***η* (%)**	***F* (Hz)**	**Ref**
BNT-BT-La	300	3.3	89	500	[60]
BKT-BT-NN	320	5.2	80	100	[10]
KNN-BZT	400	3.8	91.4	100	[16]
NKSN-SZ-BNZ	300	3.3	86	100	[61]
NN-CT	200	1.3	94	100	[62]
BNST-BMN	300	3.25	94	200	[63]
BNT-BAT-CT-BS	200	1.7	86	200	[64]
BNT-NN-SBS	300	2.5	83	600	[65]
BNT-BT-CTT	300	3.6	92	200	[66]
KNN-H	400	4.7	88	300	[53]
BF-ST	350	3.8	91	100	[59]
BKT-CT	**350**	**3.49**	**91.33**	**500**	**This work**

References

1. Z. Hu, B. Ma, R. E. Koritala and U. Balachandran, *Appl. Phys. Lett.*, 2014, **104**, 263902.
2. I. Fujii, S. Trolier-McKinstry and C. Nies, *J. Am. Ceram. Soc.*, 2011, **94**, 194-9.
3. L. Wu, X. Wang, Z. Shen and L. Li, *J. Am. Ceram. Soc.*, 2017, **100**, 265-75.
4. H. Pan, J. Ma, J. Ma, Q. Zhang, X. Liu, B. Guan, L. Gu, X. Zhang, Y.-J. Zhang, L. Li, Y. Shen, Y.-H. Lin and C.-W. Nan, *Nat. Commun.*, 2018, **9**, 1813.
5. F. Li, T. Jiang, J. Zhai, B. Shen and H. Zeng, *J. Mater. Chem. C*, 2018, **6**, 7976-81.
6. F. Li, X. Hou, T. Li, R. Si, C. Wang and J. Zhai, *J. Mater. Chem. C*, 2019, **7**, 12127-38.
7. F. Li, R. Si, T. Li, C. Wang and J. Zhai, *Ceram. Int.*, 2020, **46**, 6995-8.
8. Q. Yang, M. Zhu, Q. Wei, M. Zhang, M. Zheng and Y. Hou, *Chem. Eng. J.*, 2021, **414**, 128769.
9. Y. Wei, N. Zhang, C. Jin, J. Shen, J. Xie, Z. Dai, L. Hu, Y. Zeng and Z. Jian, *Mater. Design*, 2021, **207**, 109887.
10. L. Chen, F. Long, H. Qi, H. Liu, S. Deng and J. Chen, *Adv. Funct. Mater.*, 2022, **32**, 2110478.
11. Z. Niu, P. Zheng, Y. Xiao, C. Luo, K. Zhang, J. Zhang, L. Zheng, Y. Zhang and W. Bai, *Mater. Chem.*, 2022, **24**, 100898.
12. X. Wang, Y. Fan, B. Zhang, A. Mostaed, L. Li, A. Feteira, D. Wang, D. C. Sinclair, G. Wang and Reaney, *J. Eur. Ceram. Soc.*, 2022, **42**, 7381-7.
13. H. Wang, E. Li, K. Wei, H. Li, M. Xing and C. Zhong, *ACS Appl. Mater. Inter.*, 2022, **14**, 54021-33.
14. Y. Li, Z. Chang, M. Zhang, M. Zhu, M. Zheng, Y. Hou, Q. Zhou, X. Chao, Z. Yang, H. Qi, J. Chen, Z. Liu, H. Huang, X. Ke and M. Sui, *Small*, 2024, **20**, 2401229.
15. C. Li, J. Liu, W. Bai, S. Wu, P. Zheng, J. Zhang, Z. Pan and J. Zhai, *J. Mater. Chem. A*, 2022, **10**, 9535-46.
16. F. Yan, X. Zhou, X. He, H. Bai, S. Wu, B. Shen and J. Zhai, *Nano Energy*, 2020,

75, 105012.

17. D. Li, D. Zhou, D. Wang, W. Zhao, Y. Guo and Z. Shi, *Adv. Funct. Mater*., 2022, **32**, 2111776.
18. J. Zhao, Z. Pan, L. Tang, Y. Shen, X. Chen, H. Li, P. Li, Y. Zhang, J. Liu and J. Zhai, *Mater. Today Phys*., 2022, **27**, 100821.
19. S. Ji, Q. Li, D. Wang, J. Zhu, M. Zeng, Z. Hou, Z. Fan, X. Gao, X. Lu, Q. Li and J.-M. Liu, *J. Am. Ceram. Soc*., 2021, **104**, 2646-54.
20. H. Qi, A. Xie, A. Tian and R. Zuo, *Adv. Energy Mater*., 2020, **10**, 1903338.
21. X. Zhang, D. Hu, Z. Pan, X. Lv, Z. He, F. Yang, P. Li, J. Liu and J. Zhai, *Chem. Eng. J*., 2021, **406**, 126818.
22. Q. Hu, Y. Tian, Q. Zhu, J. Bian, L. Jin, H. Du, D. O. Alikin, V. Y. Shur, Y. Feng, Z. Xu and X. Wei, *Nano Energy*, 2020, **67**, 104264.
23. R. Kang, Z. Wang, W. Liu, L. He, X. Zhu, P. Shi, X. Zhang, L. Zhang and X. Lou, *ACS Appl. Mater. Inter*., 2021, **13**, 25143-52.
24. F. Yan, K. Huang, T. Jiang, X. Zhou, Y. Shi, G. Ge, B. Shen and J. Zhai, *Energy Storage Mater*., 2020, **30**, 392-400.
25. X. Qiao, F. Zhang, D. Wu, B. Chen, X. Zhao, Z. Peng, X. Ren, P. Liang, X. Chao and Z. Yang, *Chem. Eng. J*., 2020, **388**, 124158.
26. T. Wei, K. Liu, P. Fan, D. Lu, B. Ye, C. Zhou, H. Yang, H. Tan, D. Salamon, B. Nan and H. Zhang, *Ceram. Inter*., 2021, **47**, 3713-9.
27. H. Chen, J. Shi, X. Chen, C. Sun, F. Pang, X. Dong, H. Zhang and H. Zhou, *J. Mater. Chem. A*, 2021, **9**, 4789-99.
28. Y. Pu, W. Wang, X. Guo, R. Shi, M. Yang and J. Li, *J. Mater. Chem. C*, 2019, **7**, 14384-93.
29. T. Ouyang, Y. Pu, J. Ji, S. Zhou and R. Li, *Ceram. Inter*., 2021, **47**, 20447-55.
30. L. Zheng, Z. Niu, P. Zheng, K. Zhang, C. Luo, J. Zhang, N. Wang, W. Bai and Y. Zhang, *Mater. Today Energy*, 2022, **28**, 101078.
31. Q. Wang, P.-M. Gong and C.-M. Wang, *Ceram. Inter*., 2020, **46**, 22452-9.
32. D. Hu, Z. Pan, X. Tan, F. Yang, J. Ding, X. Zhang, P. Li, J. Liu, J. Zhai and H. Pan, *Chem. Eng. J*., 2021, **409**, 127375.

33. X. Li, X. Chen, J. Sun, M. Zhou and H. Zhou, *Ceram. Inter*., 2020, **46**, 3426-32.
34. H. Yang, Z. Lu, L. Li, W. Bao, H. Ji, J. Li, A. Feteira, F. Xu, Y. Zhang, H. Sun, Z. Huang, W. Lou, K. Song, S. Sun, G. Wang and D. Wang, *ACS Appl. Mater. Inter*., 2020, **12**, 43942-9.
35. J. Zhao, S. Bao, L. Tang, Y. Shen, Z. Su, F. Yang, J. Liu and Z. Pan, *J. Alloy. Compd*., 2022, **898**, 162795.
36. W. Wang, Y. Pu, X. Guo, R. Shi, M. Yang and J. Li, *J. Alloy. Compd*., 2020, **817**, 152695.
37. C. Li, J. Liu, L. Lin, W. Bai, S. Wu, P. Zheng, J. Zhang and J. Zhai, *Small*, 2023, **19**, 2206662.
38. J. Zhang, J. Wang, D. Gao, H. Liu, J. Xie and W. Hu, *J. Eur. Ceram. Soc*., 2021, **41**, 352-9.
39. F. Si, B. Tang, Z. Fang, H. Li and S. Zhang, *J. Alloy. Compd*., 2020, **819**, 153004.
40. P. Zhao, B. Tang, F. Si, C. Yang, H. Li and S. Zhang, *J. Eur. Ceram. Soc*., 2020, **40**, 1938-46.
41. X. Kong, L. Yang, Z. Cheng and S. Zhang, *J. Am. Chem. Soc*., 2020, **103**, 1722-31.
42. Y. Ding, P. Li, J. He, W. Que, W. Bai, P. Zheng, J. Zhang and J. Zhai, *Compos. Part B: Eng*., 2022, **230**, 109493.
43. D. Li, D. Zhou, W. Liu, P. -J. Wang, Y. Guo, X. -G. Ya and H. -X. Lin, *Chem. Eng. J*., 2021, **419**, 129601.
44. Ji. H, Wang. D, Bao. W, Lu. Z, Wang. G, Yang. H, Mostaed. A, Li. L, Feteira. A, Sun. S, Xu. F, Li. D, Ma. C.-J and Liu. S.-Y, *Energy Storage Mater.* 2021, **38**, 113-20.
45. C. Zhu, Z. Cai, L. Li and X. Wang, *J. Alloy. Compd*., 2020, **816**, 152498.
46. Z. Dai, J. Xie, X. Fan, X. Ding, W. Liu, S. Zhou and X. Ren, *Chem. Eng. J*., 2020, **397**, 125520.
47. Y. Huang, C. Zhao, B. Wu and J. Wu, *ACS Appl. Mater. Inter*., 2020, **12**, 23885-95.
48. L. Zhang, L.-X. Pang, W.-B. Li and D. Zhou, *J. Eur. Ceram. Soc*., 2020, **40**,

3343-7.

49. N. Luo, K. Han, M. J. Cabral, X. Liao, S. Zhang, C. Liao, G. Zhang, X. Chen, Q. Feng, J.-F. Li and Y. Wei, *Nat. Commun*., 2020, **11**, 4824.
50. W. Cao, R. Lin, X. Hou, L. Li, F. Li, D. Bo, B. Ge, D. Song, J. Zhang, Z. Cheng and C. Wang, *Adv. Funct. Mater*., 2023, **33**, 2301027.
51. X. Kong, L. Yang, Z. Cheng and S. Zhang, *Mater*., 2020, **13**, 180.
52. Z. Sun, J. Zhang, H. Luo, Y. Yao, N. Wang, L. Chen, T. Li, C. H, H. Qi, S. Deng, L. C. Gallington, Y. Zhang, J. C. Neuefeind, H. Liu and J. Chen, *J. Am. Chem. Soc*., 2023, **145**, 6194-202.
53. L. Chen, S. Deng, H. Liu, J. Wu, H. Qi and J. Chen, *Nat. Commun*., 2022, **13**, 3089.
54. M. Zhang, H. Yang, Y. Lin, Q. Yuan and H. Du, *Energy Storage Mater*., 2022, **45**, 861-8.
55. Q. Yuan, F.-Z. Yao, S.-D. Cheng, L. Wang, Y. Wang, S.-B. Mi, Q. Wang, X. Wang and H. Wang, *Adv. Funct. Mater*., 2020, **30**, 2000191.
56. S. Li, T. Hu, H. Nie, Z. Fu, C. Xu, F. Xu, G. Wang and X. Dong, *Energy Storage Mater*., 2021, **34**, 417-26.
57. G. Liu, M. Tang, X. Hou, B. Guo, J. Lv, J. Dong, Y. Wang, Q. Li, K. Yu, Y. Yan and L. Jin, *Chem. Eng. J*., 2021, **412**, 127555.
58. M. Zhang, H. Yang, Y. Yu and Y. Lin, *Chem. Eng. J*., 2021, **425**, 131465.
59. F. Yan, H. Bai, G. Ge, J. Lin, C. Shi, K. Zhu, B. Shen, J. Zhai and S. Zhang, *Small*, 2022, **18**, 2106515.
60. B. Chu, J. Hao, P. Li, Y. Li, W. Li, L. Zheng and H. Zeng, *ACS Appl. Mater. Inter*., 2022, **14**, 19683-96.
61. A. Xie, J. Fu, R. Zuo, X. Jiang, T. Li, Z. Fu, Y. Yin, X. Li and S. Zhang, *Adv. Mater*., 2022, **34**, 2204356.
62. A. Xie, J. Fu, R. Zuo, C. Zhou, Z. Qiao, T. Li and S. Zhang, *Chem. Eng. J*., 2022, **429**, 132534.
63. X. Li, Y. Cheng, F. Wang, Q. Xu, Y. Chen, L. Xie, Z. Tan, J. Xing and J. Zhu, *Chem. Eng. J*., 2022, **431**, 133441.

64. Y. Ding, W. Que, J. He, W. Bai, P. Zheng, P. Li, J. Zhang and J. Zhai, *J. Eur. Ceram. Soc*., 2022, **42**, 29-139.
65. C. Zhang, W. Xiao, F. Zeng, D. Su, K. Du, S. Qiu, G. Fan, W. Lei, H. Zhang, S. Jiang, J.-M. Wu and G. Zhang, *J. Mater. Chem*. *A*, 2021, **9**, 10088-94.
66. T. Li, X. Jiang, J. Li, A. Xie, J. Fu and R. Zuo, *ACS Appl. Mater. Inter*., 2022, **14**, 22263-9.